Supplemental Data

Oscillatory Transepithelial H^+ Flux Regulates a Rhythmic Behavior in *C. elegans*

Jason Pfeiffer, David Johnson, and Keith Nehrke

Supplemental Experimental Procedures

Strains

Standard culture techniques were used to maintain nematodes at 20°C [S1]. The wild-type strain is Brisol N2. All of the mutants described in this work have been outcrossed at least three times prior to use. The reporters used in this work include the pH-sensitive GFP variant pHluorin expressed exclusively in the intestinal cells and used to measure pHi (P*nhx-2*::pHluorin); pHluorin fused as a chimera to the targeting domain(s) of PAT-3 and expressed at the basolateral membrane of posterior intestinal cells to measure extracellular pH (P*nhx-7*::PAT-3::pHluorin); and the rescue construct pJP113nhx-7 (P*nhx-7*::NHX-7::GFP). The strains are: RB793 *nhx-7(ok583)*X; KWN1 *pha-1(e2123ts)*III; *him-5(e1490)*V; rnyEx001[P*nhx-2*::YC6.1,*pha-1*(+)]; KWN26 *pha-1(e2123ts)*III; rnyEx006[P*nhx-2*::pHluorin, *pha1*(+)]: KWN27 *itr-1(sa73)*IV; *pha-1 (e2123ts)*III; rnyEx006; KWN28 *unc-43(sa200)*IV; *pha-1 (e2123ts)*III; rnyEx006; KWN29 *nhx-7(ok583)*X; *pha-1 (e2123ts)*III; rnyEx006; KWN30 *pha-1(e2123ts)*III; rnyEx009[P*nhx-7*::PAT-3::pHluorin, *pha-1*(+)]; KWN31 *nhx-7(ok583)*X; *pha-1(e2123ts)*III; rnyEx009; KWN33 *nhx-7(ok583)*X; *pha-1(e2123ts)*III; rnyEx011 [P*nhx-7*::NHX-7::GFP].

Constructs and Microinjections

The construction of the intestinal pHluorin expression vector pIA5nhx-2 for measuring pHi has been described [S2], as has the P*nhx-7*::NHX-7::GFP rescue vector pJP113nhx-7 [S3]. To measure extracellular pH, a vector expressing the pHlourin pH sensor as a chimera with the β integrin subunit PAT-3 was created. First, PAT-3 cDNA was PCR amplified from the Fire lab expression vector pPD122.39 with primers that contained Acc65I (5′) and NotI (3′) nonsequence encoded tags for cloning purposes. The digested PCR product was cloned into the complementary sites in the vector pFH6.II [S4] to create pDJ1. The ratiometric pHluorin [S5] cDNA was then PCR amplified from the vector pIA5nhx-2 with 5′ and 3′ BspE1 tags and cloned into the BspE1 site of pDJ1 to create pDJ2. Finally, a 4 kb NheI-SacII fragment from pJP108nhx-7 [S3] containing the *nhx-7* promoter was cloned into pDJ2 to create pDJ3. The RNA interference vector pRNAi-nhx-2 has been described [S2] and the vector pRNAi-cmd-1 contains a 1074 nt genomic PCR fragment amplified with the primers 5′- CACGGATCCGGTATTCATCATTGTTTACG-3′ and 5′-CACTC TAGATGAGAGAAAAGGTGTTGGTGATT-3′ and cloned into the BamHI-XbaI sites of the vector pPD129.36 (Courtesy of A. Fire, Stanford University). All PCR-amplified fragments were fully sequenced.

To create transgenic strains containing extrachromosomal arrays, constructs were mixed with pCL1, which codes for *pha-1*(+) [S6], at 75 μg/ml each in high-potassium injection buffer, then coinjected into the gonad of *pha-1(e2131ts)III* mutants (and occasionally *pha-1(e2131ts)III; him-5(e1490)*V mutants), as described [S7]. After 4 days at 22°C, F1 progeny were examined for germline transmission.

RNA Interference

The bacterial strain HT115, which codes for T7 RNA polymerase under the control of the lac repressor, was transformed with pRNAinhx-2. Freshly transformed bacteria were grown to mid-log phase at 37°C and induced for 1 hr with 1 mM IPTG. After 5-fold concentration, 80 μl of bacteria was added to the surface of 35 or 60 mm NGM agar or agarose plates supplemented with cholesterol and 0.1 mM IPTG. The plates were allowed to dry for 2 days prior to use. L3 larvae were placed onto the RNAi plates for 36 hr prior to being moved to a fresh plate, where they were allowed to lay eggs. These F1 generation progeny were then used for further experiments.

Behavioral Assays

Except where specified, defecation was assessed at room temperature (20°C–22°C) in young adults that were actively feeding as judged by pharyngeal pumping. The execution of the DMP was followed with a Nikon SMZ800 stereo-microscope, and the cycle time was calculated as the period between successive principle contractions, where pBoc was strong and followed in sequence by aBoc and expulsion. Statistical significance was determined by an unpaired Student's t test.

Contractions of the body wall muscle during pBoc were quantified by first digitally recording visible light images at 10 Hz of worms on plates during execution of the DMP. The images were acquired on a Nikon TE2000 inverted microscope with the rig described below and analyzed with TILLvisION software. The perimeter length of the body from the tail to the vulva (P) was determined in individual frames at points in the movie immediately prior to pBoc and at the point of maximum contraction, approximately 2 s later. The contraction strength was defined as $[1 - (P_{contracted}/P_{relaxed})]$ and generally fell within a range of 0.11–0.15 for wild-type worms (n = 10). The data in Figure S2 has been normalized as a percentage of the average contraction in the wild-type controls.

The duration of the contraction is the time over which visible compression of the intestinal lumen persists.

Calcium and pH Imaging

Live behaving worms were imaged on NGM agarose plates. To compensate for the lack of physical restraints, the worms were kept in the center of the field of view manually during the imaging process via a stage controller. In general, optical recordings were acquired on a Nikon TE2000U inverted microscope (10× Plan Apo air objective, 0.5NA) that was coupled to a monochromatic light source (Polychrome IV, TILL Photonics), CCD camera detection system (Cooke Sensicam) ± beamsplitter (Optical Insights) at a frame rate between 4 and 10 Hz. TILLvisION software was run for both acquisition and analysis.

For measuring Ca^{2+} with YC6.1, the acquisition conditions were as follows: dual emissions at 480 and 535 nm were captured in a single frame through the beamsplitter after a 40 ms exposure (2 × 2 binning) at 435 nm. FRET was calculated by splitting the dual emission image into individual channels, then generating an emission ratio (R) image overlay after pixel-by-pixel background subtraction and thresholding. By setting all values that were not above the threshold after background subtraction in the single channel emission images to zero prior to generating the ratio overlay, only

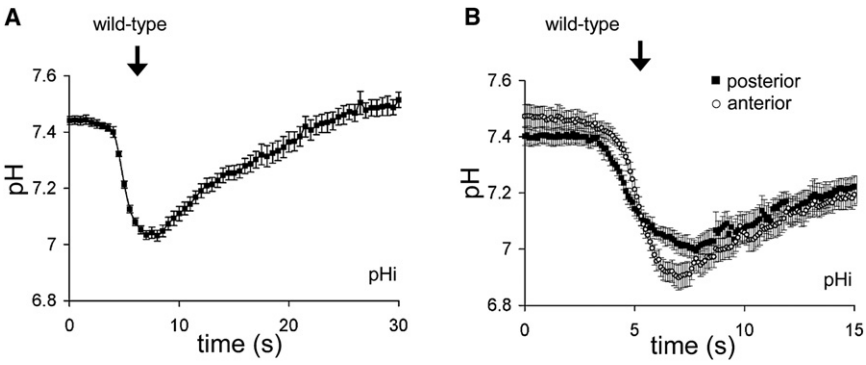

Figure S1. Intestinal pHi Dynamics and Wave Propagation

(A) Six wild-type worms were imaged for five cycles apiece. The resulting pHi oscillations were normalized to pBoc (arrow) and plotted as an average (n = 6) versus time. The error shown is the standard error of the mean (SEM).

(B) Representation of single-cycle pHi dynamics in the posterior- and anterior-most intestinal rings. The imaging was done at 10 Hz to facilitate analysis of pHi wave propagation. Values were obtained from regions of interest drawn around the posterior and anterior cell rings, as indicated, and updated manually as the worms (n = 5) moved. The error plotted is the standard deviation (SD).

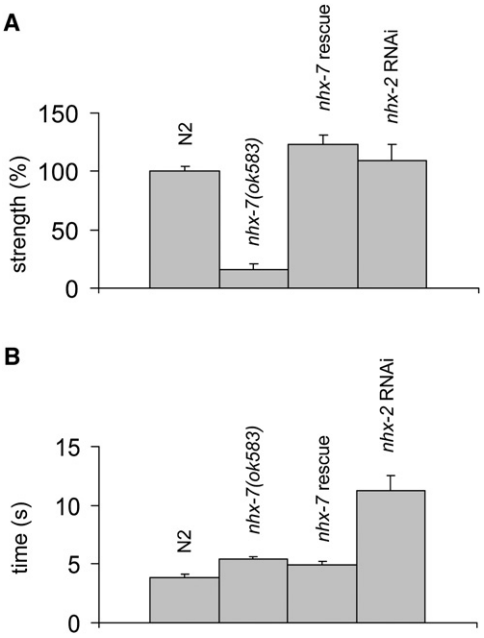

Figure S2. pBoc Contraction Strength and Duration

Transmitted light images were recorded at 4 Hz during defecation. The worms are control wild-type, *nhx-7(ok583)* mutants, *nhx-7* mutants rescued by a P*nhx-7*::NHX-7::GFP transgene, and *nhx-2(RNAi)*.

(A) Contraction strength was determined by dividing the perimeter of the posterior body preceding pBoc by its length at the apex of pBoc.

(B) The duration of pBoc was assessed post hoc from the same recordings. The NHX-7 transgene can restore normal contraction strength in the *nhx-7(ok583)* mutant, and loss of NHX-2 increases the duration of the contraction. The error bars are the standard deviations (n = 7–10 worms).

the high-intensity fluorescent signals in the intestine contributed to R. In general, we used a threshold value that was twice the average background signal. Changes in the fluorescent emission ratios (R/R_0) over time were averaged throughout the entire intestine as an indicator of global Ca^{2+} flux. To measure Ca^{2+} wave propagation, R/R_0 was determined in single intestinal cell rings over time. The cells were identified and regions of interest (ROI) were defined with the 435 nm single channel fluorescent emission image as a guide. The ROI were updated in successive images to account for locomotion/movement of the worm. pBOC was denoted post hoc from the image series as a posterior body wall muscle contraction that caused compression of the intestine, and aBOC as a depression of the pharynx into the lumen of the intestine, which displaces the anterior-most segment of int-1. Expulsion, which consists of a short (<1 s) contraction of the enteric muscles, was less apparent, but could be observed at higher frame rates (i.e., >8 Hz).

For pH measurements, pHluorin emissions were measured (without the beamsplitter) at 535 nM after sequential 10 ms excitations (2 × 2 binning) at 410 and 470 nM. The single channel 410 nm and 470 nm images were aligned and a pixel-by-pixel ratio map was created after background subtraction on each channel and thresholding, as described above. The pHluorin signal was relatively homogeneous throughout the intestine, and the TILL monochromator took only 3 ms to switch between excitation wavelengths, so ratio artifacts caused by the worm moving between the 410 nm and 470 nm acquisitions were minimized. Our analysis of pH dynamics and pH wave propagation was similar to that described for Ca^{2+}, except that the 410/470 nm ratios were converted to absolute pH values. For this, the intestinal cells of worms attached to a glass coverslip under perfusion were allowed to extrude via gently slicing the cuticle with a 32-gauge needle immediately posterior to the pharyngeal-intestinal valve. In situ calibration was performed by the high K^+/nigericin technique [S8]. For the extracellular pH indicator, neither K^+ nor nigericin were necessary for calibration, and the reporter was inherently sensitive to buffer pH.

The vital dyes Oregon Green 488 Dextran (1 μM) or BCECF-AM (1 μM) were fed to the worms in S-media supplemented with OP50 bacteria for 1 hr at room temperature. The worms were then pipetted onto an NGM-agarose plate for imaging. Image acquisition, analysis, and calibration were as described for pHluorin, except that the dual excitation wavelengths for these two compounds were 490 nm and 440 nm. Calibrations were performed as described for the biosensors.

Confocal micrographs were acquired on a Nikon TE300 microscope coupled to a C1 confocal system with 488 nm or 543 nm laser illumination, a 40× Plan Apo objective, and a 30 μm pinhole.

Supplemental References

S1. Brenner, S. (1974). The genetics of *Caenorhabditis elegans*. Genetics *77*, 71–94.

S2. Nehrke, K. (2003). A reduction in intestinal cell pHi due to loss of the *Caenorhabditis elegans* Na^+/H^+ exchanger NHX-2 increases life span. J. Biol. Chem. *278*, 44657–44666.

S3. Nehrke, K., and Melvin, J.E. (2002). The NHX family of Na^+/H^+ exchangers in *Caenorhabditis elegans*. J. Biol. Chem. *277*, 29036–29044.

S4. Hagen, F.K., and Nehrke, K. (1998). cDNA cloning and expression of a family of UDP-N-acetyl-D-galactosamine:polypeptide N-acetylgalactosaminyltransferase sequence homologs from *Caenorhabditis elegans*. J. Biol. Chem. *273*, 8268–8277.

S5. Miesenbock, G., De Angelis, D.A., and Rothman, J.E. (1998). Visualizing secretion and synaptic transmission with pH-sensitive green fluorescent proteins. Nature *394*, 192–195.

S6. Granato, M., Schnabel, H., and Schnabel, R. (1994). *pha-1*, a selectable marker for gene transfer in *C. elegans*. Nucleic Acids Res. *22*, 1762–1773.

S7. Mello, C.C., Kramer, J.M., Stinchcomb, D., and Ambros, V. (1991). Efficient gene transfer in *C. elegans*: extrachromosomal maintenance and integration of transforming sequences. EMBO J. *10*, 3959–3970.

S8. Thomas, J.A., Buchsbaum, R.N., Zimniak, A., and Racker, E. (1979). Intracellular pH measurements in Ehrlich ascites tumor cells utilizing spectroscopic probes generated in situ. Biochemistry *18*, 2210–2218.

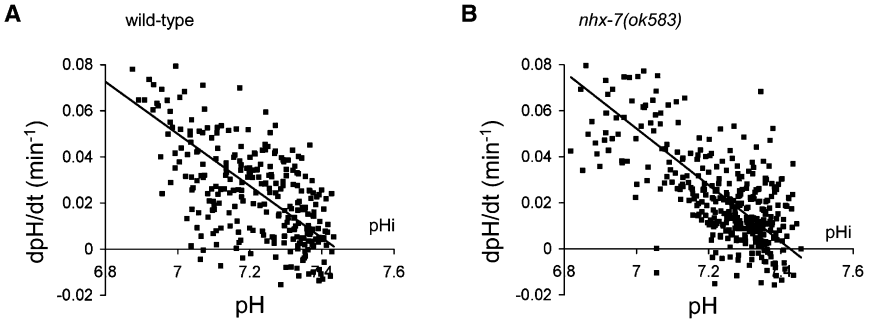

Figure S3. Intracellular pHi Recovery as a Function of NHX-7

Scatter plots of the rate of recovery (dpHi/dt) as a function of pHi after defecation in control (A) and *nhx-7(ok583)* mutant (B) worms (n = 3). These data suggest (p value > 0.05) that NHX-7 does not contribute significantly to pHi recovery.

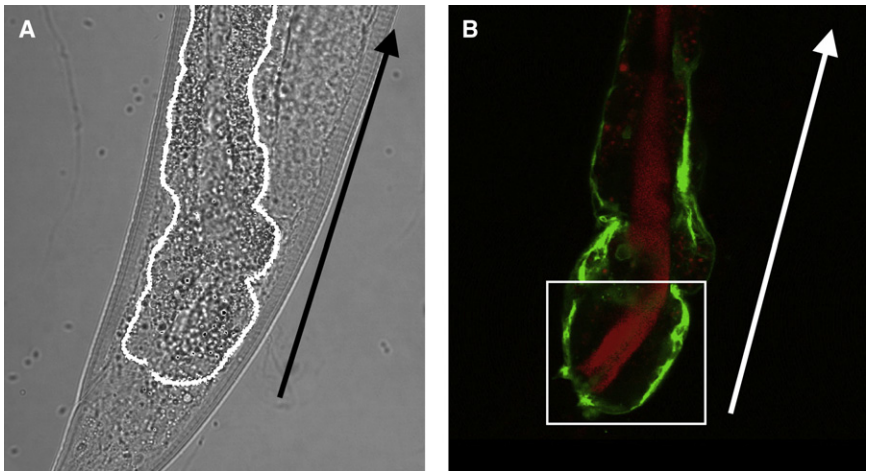

Figure S4. An Extracellular pH Sensor Expressed at the Basolateral Membrane

Transmission (A) and fluorescence confocal (B) images from an adult *nhx-7(ok583)* mutant expressing an P*nhx-7*::PAT-3::pHluorin transgene in the posterior epithelial cells of the intestine. The intestinal basolateral membrane is outlined in white in the transmission image. The gut granules in the intestinal cytoplasm are autofluorescent in the red spectrum, as are the bacteria in the intestinal lumen, while pHluorin fluoresces green; the *nhx-7(ok583)* mutant is slightly constipated, and the fluorescent green-red overlay in (B) demonstrates a clear distinction between the lumen, the cytoplasm, and the basolateral membrane where the reporter protein resides. The arrows point from the posterior toward the anterior end of the intestine. The white box in (B) indicates the posterior-most intestinal cells.

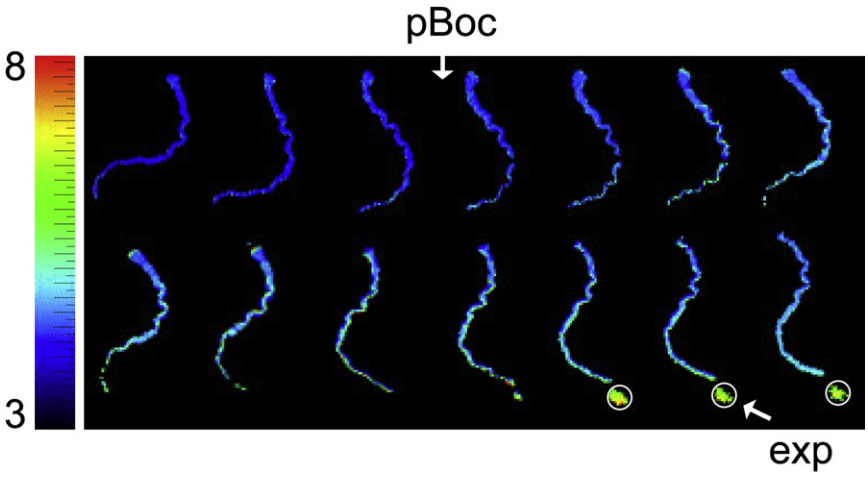

Figure S5. Reduced Luminal Alkalinization in *nhx-2(RNAi)* Worms during Defecation

Representative frames from a time-lapse acquisition of pH changes in the lumen of wild-type worms treated with *nhx-2* RNAi. Consecutive frames obtained at 2 Hz are shown. Wild-type worms were fed dextran coupled to the pH-sensitive vital dye Oregon Green 488. The fluorescent ratios (490 nm/440 nm dual excitation, 535 nm emission) obtained by imaging live worms during defecation were mapped to a rainbow palette, as indicated. The execution of pBoc and explusion are denoted. The plate is approximately pH 6, and the expelled luminal contents, which are normally quite acidic in these worms, reflect the pH of the plate, as shown by white circles. The worm is oriented with the anterior facing upwards.

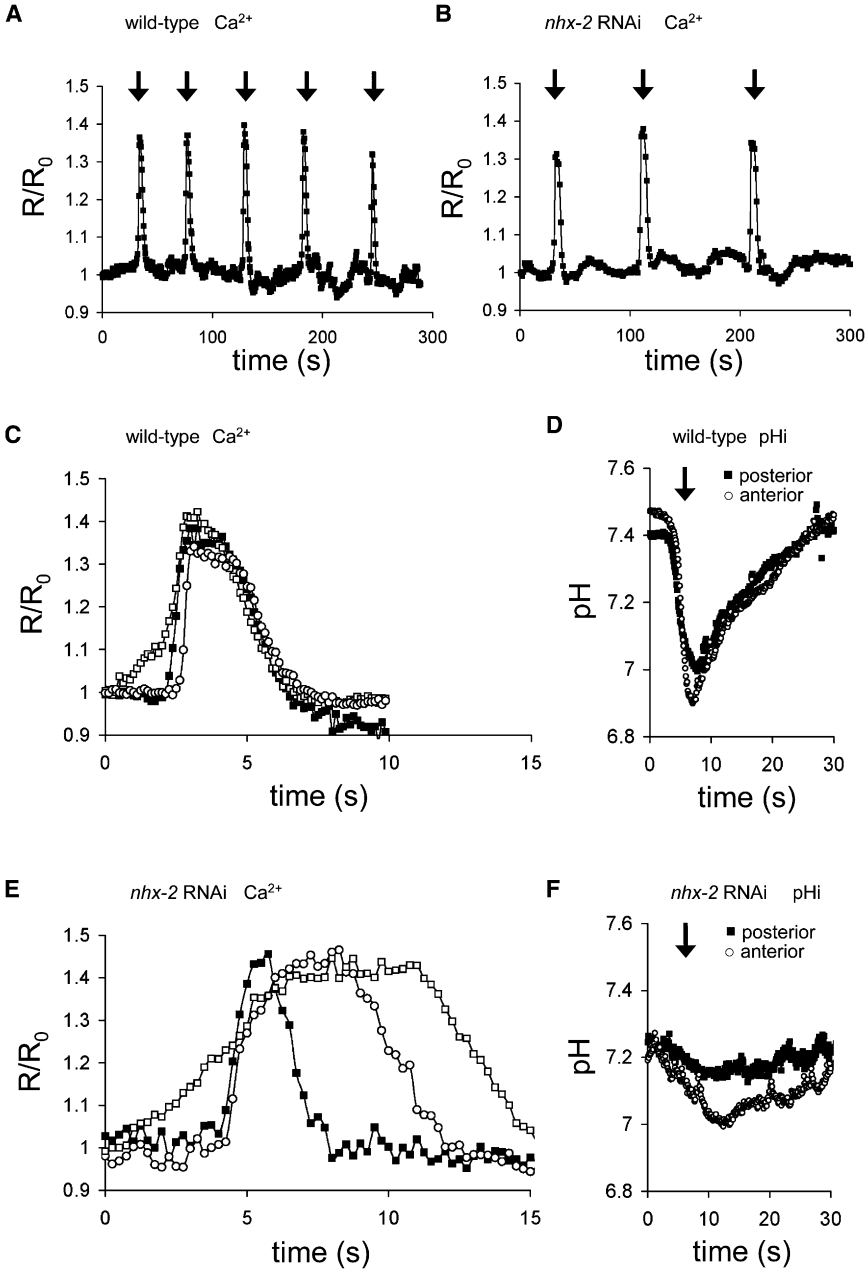

Figure S6. Ca^{2+} and pH Wave Propagation in *nhx-2(RNAi)* Worms

Ca^{2+} (A, B, C, E) or pH (D, F) measurements were obtained from the entire intestine (A, B) or individual regions of interest (C–F) in either control (A, C, E) or *nhx-2* RNAi-treated (B, D, F) worms, as indicated. The Ca^{2+} traces in (C) and (E) depict changes in the anterior intestinal cell ring (open squares), the posterior cell ring (closed squares), and the midintestinal cell ring int5 (open circles). Because Ca^{2+} is elevated in the anterior cell ring prior to wave propagation during defecation, as shown, the time between a 10% increase in R/R_0 in the posterior intestine versus the midintestinal ring int5 more closely represents the wave propagation rate. This rate is not obviously reduced by *nhx-2* RNAi, though the amount of time required for Ca^{2+} clearance is extended at the anterior of the intestine. Unlike Ca^{2+}, the pH wave initiates solely in the posterior intestinal ring and propagates forward. Similar to Ca^{2+}, however, the rate of pH wave propagation itself does not appear to depend upon normal NHX-2 activity, and the overall acidification rate is reduced in both the posterior and anterior cells.

Table S1. Quantitative Analysis of pH and Ca^{2+} Oscillations during Defecation

Allele	Control N2	*nhx-7(ok583)*	Control N2
RNAi	N/A	N/A	*nhx-2*
pBoc Period (s)	44.3 ± 5.1	52.0 ± 4.7	86.7 ± 4.7*
Ca^{2+} Period (s)	55.1 ± 3.0	52.9 ± 2.9	79.3 ± 11.8*
pHi Period (s)	49.7 ± 8.2	48.1 ± 7.5	81.3 ± 16.3*
pHo Period (s)	54.1 ± 7.8	54.2 ± 4.6	95.0 ± 9.0*
pHl Period (s)	47.1 ± 5.6	47.2 ± 8.6	71.3 ± 3.8*
pHi Resting	7.40 ± 0.05	7.39 ± 0.04	7.22 ± 0.05*
ΔpHi	0.40 ± 0.05	0.44 ± 0.06	0.16 ± 0.04*
pHo Resting	7.29 ± 0.11	7.32 ± 0.08	7.31 ± 0.12
ΔpHo	0.97 ± 0.12	0.19 ± 0.05*	1.02 ± 0.19
pHl Resting	4.05 ± 0.06	4.10 ± 0.11	4.10 ± 0.08
ΔpHl	1.98 ± 0.10	1.91 ± 0.21	0.53 ± 0.29*

This table contains mean values for intestinal cytoplasmic pH (pHi), extracellular pH at the basolateral cell surface (pHo), luminal pH (pHl), or Ca^{2+} oscillations, as indicated (n = 5–13 individual worms). In the absence of a sensor, the defecation period was assessed visually with a stereo-dissecting microscope. The period for pH and Ca^{2+} sensor experiments was derived post hoc from the fluorescent time-lapse acquisitions based upon mean oscillation frequencies. For the purposes of this analysis, the entire intestine was treated as single region of interest and the values reported here represent average intestinal measurements. For pH oscillations, the mean resting pH was taken immediately prior to defecation. The pHi reported here is somewhat lower than that observed in anesthetized worms, probably because of a slow rate of intracellular acidification that occurs between defecation cycles. N/A is not applicable; the error is the standard deviation. Statistical significance was determined by Student's t test.
*$p < 0.01$.